CCUS: 4000338

Carbon Storage Feasibility Assessment of the Vermilion Leasing Block, Central Gulf of Mexico, USA: Opportunities for Depleted Field and Saline Reservoir Storage

Lars Koehn[1], Matthew Tascione*[1], Abduljeleel Ajibona[2], Ethan Conley[1], Salman Karim*[2], John Ogunleye[1], Uzezi Orivri*[2], Akash Talapatra[2], 1. Department of Geosciences Virginia Polytechnic Institute and State University, 2. Department of Mining and Minerals Engineering, Virginia Polytechnic Institute and State University.

This paper was prepared for presentation at the Carbon Capture, Utilization, and Storage conference held in Houston, TX, 11-13 March.

Abstract

The Bureau of Energy Management (BOEM) has assessed the Vermilion Leasing Block in the Central Gulf of Mexico continental shelf for carbon storage potential in depleted petroleum fields. In their study, BOEM identified the 4-way closure of Vermilion 39 block as a potential storage site based on petroleum production history. Our project presents a detailed subsurface characterization of the Vermilion 39 field with numerical simulations to more accurately assess the storage performance of the field. Additionally, we propose a high-value saline reservoir storage target in the Vermilion block, that was not considered by BOEM. This potential site is located in low-dip undeformed sediments in the Vermilion blocks 55-56 and 67-68. We present both sites as high-value targets for commercial carbon storage that could be developed by operators in the region. Both sites were characterized using 3D seismic survey and well data to identify potential storage complexes and map their structure. These interpretations were then used to build geologic models and conduct numerical simulations of CO2 injection through the TOUGH3 codes. Finally, infrastructure and economic assessments were performed to determine the commercial viability of CCS projects at both sites. Numerical simulation results suggest that the 4-way closure of Vermilion 39 could potentially hold upwards of 50 million metric tons of CO2 primarily utilizing structural and stratigraphic trapping. We determined that the greatest risks at this site are in leakage through legacy wells. Simulation results suggest that the saline reservoir storage play could also store 50 million metric tons of CO2 utilizing capillary and residual trapping to stabilize the post-injection CO2 plume. At this location, the greatest risks are in the reservoir quality of the target units. Our results indicate that the sites selected could store commercially viable volumes of captured CO2, offsetting the cost of transport and capture, and potentially running a profit through currently available 45Q tax credits. We present two high-

value targets for commercial carbon storage development in the Gulf of Mexico including a depleted reservoir play and a novel saline reservoir play. We present this research to encourage further development of commercial carbon storage in the Gulf of Mexico at these sites in the Vermilion block or at other sites with similar geology.

Introduction

Carbon capture utilization and storage (CCUS) is a strategy for reducing greenhouse gas emissions that is rapidly being adopted globally to mitigate CO_2 emissions from petroleum related processes and other heavy industries. In the United States, the Gulf of Mexico is an extremely promising region for CCS development due to its high estimated storage capacity, the abundance of subsurface data and its proximity to major CO_2 emitting facilities (NETL, 2015). While there are no presently operating commercial CCS projects in the offshore Gulf of Mexico, previous projects have demonstrated the feasibility of offshore CO_2 storage, including Sleipner in the North Sea (Furre et al., 2017) and Snøhvit in the Barents Sea (Hansen et al., 2013). Additionally, the Bureau of Ocean Energy Management (BOEM) has conducted preliminary investigations to assess depleted petroleum fields in the Gulf of Mexico for carbon storage. BOEM identified nine fields as tier 1 priority targets and of these the Vermilion leasing area contains the greatest number of identified reservoirs (Alonso et al., 2022). Our project builds on this past work by performing a thorough investigation of the feasibility of CO_2 storage at two sites in the Vermilion leasing block and demonstrating with geophysical and numerical modeling analysis that this location has high suitability for commercial CCS development.

Both the Gulf of Mexico in general, and the Vermilion block in particular, have depositional geologies suited for storing large volumes of injected CO_2. Sediment deposition and salt deformation has been ongoing in the Gulf of Mexico since the late Cretaceous with the Mississippi River acting as the primary source of sediment (Ewing and Galloway, 2019). The dynamics of salt, sediment loading, and structural systems are interconnected and impact the formation of mini basins and the migration of hydrocarbons (Sarwar, 2006). The impermeable nature of salt directs the migration of hydrocarbons along salt body edges and associated faults, influencing the distribution of hydrocarbon seep sites. These salt domes could also push up through overlying sedimentary layers, creating traps that have historically held large volumes of oil and gas but could also potentially hold injected CO_2.

The focus area for this project is situated within the Upper Miocene Sequence of the Gulf of Mexico based on its approximate depth at pressure and temperature conditions suitable for storing CO_2 in a dense super-critical state. The Upper Miocene Sequence represents the thinnest segment (~375-700 ft) among the ten third-order sequences in the area as identified by Hentz and Zeng (2003) and is divided into three sections. The upper section typically consists of two to five third-order sequences (~30 – 200 ft thick), primarily comprising progradational units of thicker shales and sandstone. Secondly, the middle section is locally thick (~35 – 70 ft) and is characterized by upward-fining, retrogradational, shale-dominated units. The lowest section contains a succession of 1-3 aggradational (~40 – 130 ft thick) or progradational (~25 – 80 ft thick) units. The Upper, Lower, and Middle Miocene distal third-order sequences primarily comprise lowstand prograding-wedge, slope-fan, and basin-floor-fan deposits. The depth to the local highstand systems tract (HST) is ~ 6000 ft (with a thickness of ~200 ft) and 6200 ft to the maximum flooding surface (MFS). The depth to the transgressive systems tracts (TST) is around 6200 ft (with a thickness of ~200 ft), and 6400 ft (with a thickness of ~700 ft) to the lowstand systems tracts (LST) in the interval of interest (Hentz and Zeng, 2003) (Figure 1).

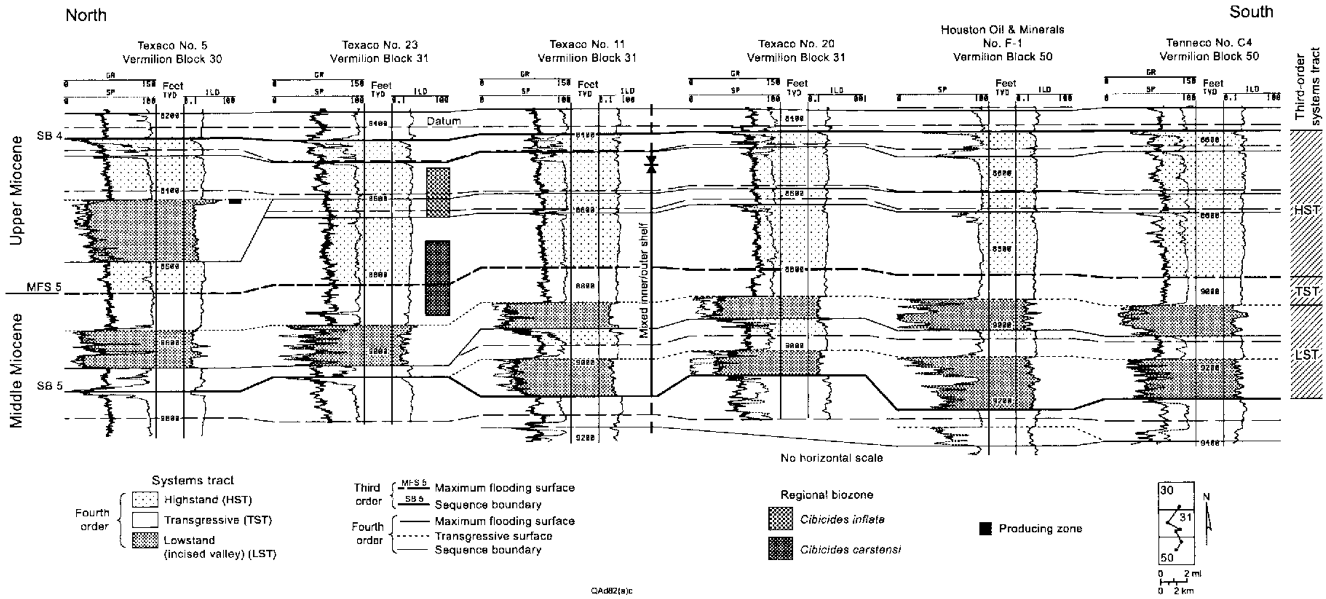

Figure 1. Medial third-order sequence 5 (middle and upper Miocene) dip cross section of the Starfak field located adjacent to the Vermilion study area. The Biozone 'boxes' describe the vertical variation in the top of each zone across the wells that contain fossil data. Paleobathymetric interpretations rely on the analysis of benthic fossil assemblages. From Hentz and Zeng (2003).

Initial screenings of the Vermilion block led to the identification of two prospects for further investigation. The first is a depleted petroleum field centered around Vermilion leasing block #39. The second is an un-penetrated saline aquifer section located in Vermilion leasing blocks #55-56 and #67-68. Target reservoirs and seals for CO_2 injection as well as major structural features and faults were identified for both prospects using 3D seismic reflection data. These mapped features were then used to build geologic models and conduct numerical simulations in order to assess their feasibility for commercial CO_2 storage. Our results indicate that both the depleted field prospect and the saline field prospect have high potential for securely storing injected CO_2 at commercially viable scales.

Methods

Within the Vermillion study area, a comprehensive selection process was undertaken to identify blocks, fields, and sands with characteristics suitable for CO_2 storage in depleted fields. Using data from BOEM (BOEM, 2019), the following criteria were used for selecting suitable blocks, fields, and sands for further detailed storage assessment: proximity to shore to minimize CO_2 transport pipeline distance, estimated ultimate recovery which gives indication of preliminary storage capacity, reservoirs with depth ranging from 3000-10000 ft, and sand with high permeability-thickness. Using the equation below, preliminary storage capacity estimates were made, where EUR, $B_{o,g}$, ρ_{CO2}, and E_f represents the estimated ultimate recovery, oil/gas formation volume factors, CO_2 density (assumed as 0.7tonnes/m^3) and efficiency factor respectively.

$$Storage\ Capacity = EUR * B_{o,g} * \rho_{CO2} * E_f$$

Various authors differ on what the efficiency factor of depleted petroleum fields for CO_2 storage with values ranging from 5-30% (Rasool et al., 2023) and up to 75% (Hannis et al., 2017). An efficiency factor of one (1) denotes theoretical capacity which assumes all the pore spaces filled with produced hydrocarbons are available for CO_2 storage (Iskandar and Usman, 2011; Rackley, 2017). A storage efficiency factor of 75% was used for a preliminary screening capacity estimate. The preliminary capacity assessment indicate that the Vermilion #39 block contains about eight sand reservoirs with theoretical storage capacity greater than 5million tonnes of CO_2, up to a total of 202 million tonnes (see Figure 2 below). The 7800 sand in Vermilion #39 field (VR039) was selected for further assessment as it yielded the highest theoretical storage capacity.

Field	Block/ Area	Sand	EUR Oil (mmbbl)	EUR Gas (BCF)	Storage Capacity (MMT)	Depth (TVD ftss)	Net Thickness (ft)	Poro	Perm (mD)	Initial Pressure (Psi)
VR039	VR39	07800	2.9	845.1	74.3	7,758	72	32%	1336	3,763
VR039	VR22	10200	3.6	494.1	37.7	7,889	26	30%	868	3,772
VR039	VR38	09500	3.0	438.1	33.3	8,485	19	28%	258	4,313
VR039	VR38	09700	17.2	222.4	20.4	8,450	29	29%	175	4,268
VR039	VR39	08400	0.9	173.0	13.6	9,191	18	26%	576	4,750
VR039	VR39	08000	0.5	122.1	10.9	9,131	28	27%	460	4,709
VR039	VR39	08600	0.4	72.9	6.1	9,663	15	27%	175	4,954
VR039	VR39	09400	3.4	63.6	5.4	9,728	34	27%	374	4,993

Figure 2. Sand properties, produced volumes and storage capacity estimates. Sand data is from the BOEM Atlas of Gulf of Mexico Oil and Gas Sands Data (2019).

The VR# 39 field is a mature oil and gas field located in the central Gulf of Mexico, offshore Louisiana, at a water depth of approximately 38ft. It was discovered in 1948 and began production in 1953. The field consists of 29 sands and 96 reservoirs, 85 of which are non-associated gas (NAG) reservoirs and 11 are oil reservoirs. Over its productive life, there have been 202 wells drilled and 323 completions. As of 2022, it has produced a cumulative 32.3 million barrels of oil and 2.6 trillion cubic feet of gas with remaining reserves estimate of 0.3 million barrels of oil and 3 billion cubic feet of gas (BOEM, 2019).

3D seismic reflection data were integrated with well data to refine the structural framework and identify prospective storage areas in the VR #39 field. Coherency slices illuminated a series of first-order and second-order faults that defined the #39 block. These faults had offset reservoir and seal intervals and appeared to constitute a downthrown segment in the depleted reservoir area. A four-way fault closure surrounded the downthrown segment and may be suitable for trapping CO_2 within a stacked storage complex. A broader fault network encircled the four-way closure and extended into adjacent Vermilion blocks, potentially offering additional storage opportunity. At 7700 ft depth below mudline, sharp gamma-ray and resistivity signatures corresponded to a high reflection amplitude and were interpreted to be a substantial sand unit. This sand was directly overlain by a high gamma-ray sealing shale and lay above both a secondary sand reservoir and a thick bottom shale seal. Additional wells within the 37th and 44th Vermilion blocks indicate that the storage complex extends through the broader encirclement of faults outside the four-way enclosure. This area broadly constitutes the CO_2 storage target: the 7700-7800 ft sand reservoir with an overlaying shale seal and a broad domal four-way fault-bounded structure to accumulate and trap injected CO_2.

As the prospect is a mature petroleum field, there are several legacy production wells that penetrate the intervals that we are targeting for carbon storage; therefore, we conducted a well leakage risk assessment, drawing insights from the report on the long-term integrity of abandoned wells during CO_2 storage by IEA GHG (2009). We have used the following criteria (indexes) to define the leakage risk associated with every well; current wellbore status, well age (casing integrity), wellbore deviation (which pose high leakage risk due to issues related to casing centralization, cement slumping, and increasing penetration surface within the caprock) and abandonment age.

$$Leakage\ index_{normalized} = Well\ Age_i * Abandoment\ Age_i * \ Well\ status_i * \ Deviation_i$$

We considered the following as high-risk wells: drilled over fifty (50) ago, currently unabandoned, abandoned earlier than 1996 (see the London Convention 1996 protocol in (IEA GHG, 2009) and with over 250ft deviation (MD vs TVD). A risk index 0-1 (low to high) were assigned to each of the criteria listed, from which an overall normalized risk index was calculated for each well. This risk analysis was performed for the wells in close proximity to the saline aquifer and within the VR039 field. About 50% of the 27 wells analyzed show a medium to high risk defined with a normalized risk index of 0.4 - 0.59 and 0.6 - 1 respectively. As a result, the project team also chose to investigate a potential CO_2 storage site not previously considered by BOEM that would have lower leakage risk from legacy wells, i.e., the unpenetrated saline aquifer identified in Vermilion leasing blocks #55-56 and #67-68.

Seismic reflection mapping of the saline field indicated that the area sits in a structural low with up-dip sections containing abundant petroleum resources and associated drilling. Therefore, the site was considered to have a suitable geology for CO_2 storage and only lacked petroleum accumulation due to up-dip migration of petroleum resources over geologic time. The major petroleum bearing sandstone units in the up-dip section were mapped to the structural lows, sitting between 6800 and 7400 ft below mudline. Furthermore, the prospect is bounded by two major East-West running faults.

Mapped features from the two prospects were used to build geologic models in PetraSim (RockWare, 2022) for simulation using the TOUGH3 codes (Jung et al., 2017) (Figures 3 and 4 below). Sandstone reservoir lateral permeabilities were assigned based on permeabilities from well data and range from 100 to 500 md with vertical permeability ranging from 10 to 50 md. Both models are laterally discretized in a polygonal mesh with Voronoi tessellation with grid cell areas ranging from 10,000 to 20 m^2. Vertical discretization is specified based on layer geology with values of 5-10 m in the target reservoirs. The saline field model contains 288,915 grid cells and the depleted field model contains 715,444 cells. The injection simulation comprised 25 years of constant injection at a rate of 2.0 million metric tonnes CO_2 injection per year distributed across a single sandstone reservoir in the depleted field model (Figure 3) and across two stacked sandstone reservoirs in the saline field model (Figure 4).

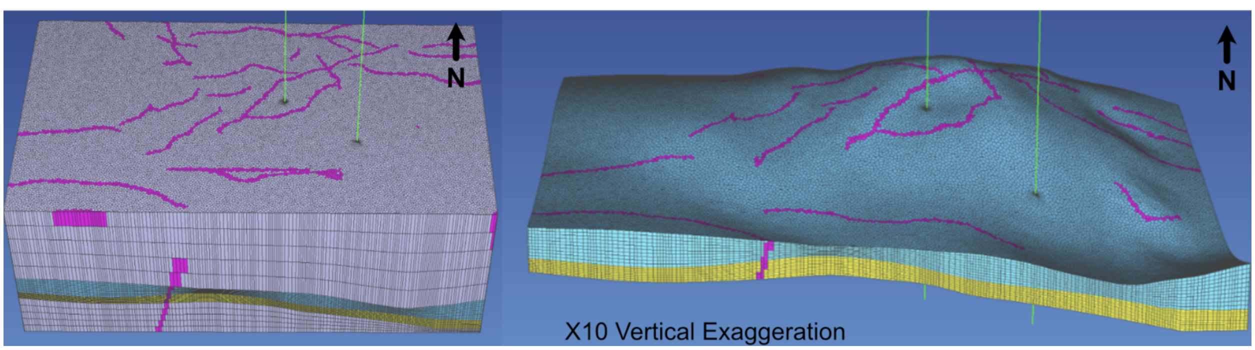

Figure 3. Depleted field model mesh. Undifferentiated overburden sediments are shown in purple, mapped shale sealing units are shown in blue, mapped sand reservoir units are shown in yellow, and grid cells that are intersected by mapped faults are shown in pink. The model is 22.2 km in length in the X direction, 13.3 km in the Y direction, and is between 2.0 km and 2.8 km in depth below mudline. The full model is shown on the left and only the reservoir-seal package and intersecting faults are shown on the right. Note the four-way structural dome at the center of the model. Two injection wells are shown in this figure, however, injection simulations presented below only utilized the injection well at the flank of the four-way structure.

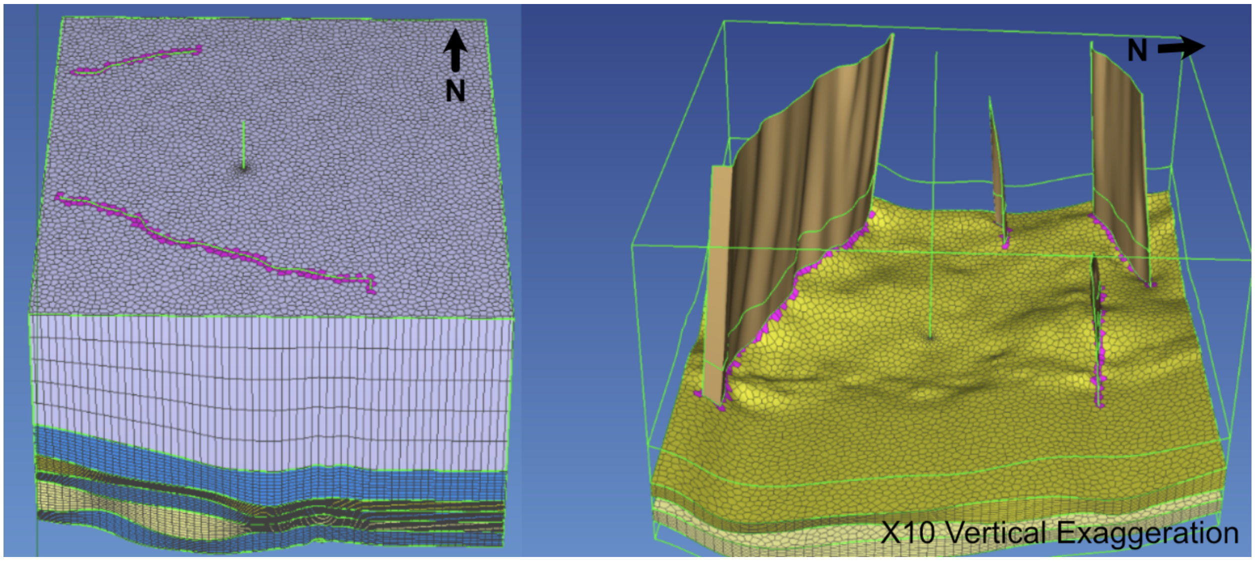

Figure 4. Saline field model mesh. Undifferentiated overburden sediments are shown in purple, mapped shale sealing units are shown in blue, mapped sand reservoir units are shown in yellow, and grid cells that are intersected by mapped faults are shown in pink. The full model is shown on the left and only the sandstone reservoirs and faults are shown on the right. The model is 7.8 km in length in the X direction, 8.2 km in the Y direction, and is between 1.8 km and 2.4 km in depth below mudline.

Results

Simulation results show that both prospects were able to securely store the 50 million tonnes of injected CO_2. Furthermore, the free gas-phase CO_2 plume did not reach major mapped faults in either scenario which may mitigate the risk of leakage through fault pathways in a CCS project. However, in both scenarios, injection-induced pressure fronts greater that 1 MPa in magnitude reached faults which could pose risks for induced seismicity or other geomechanical effects on the faults, such as fault dilation, which may increase the risk of leakage for a CCS project.

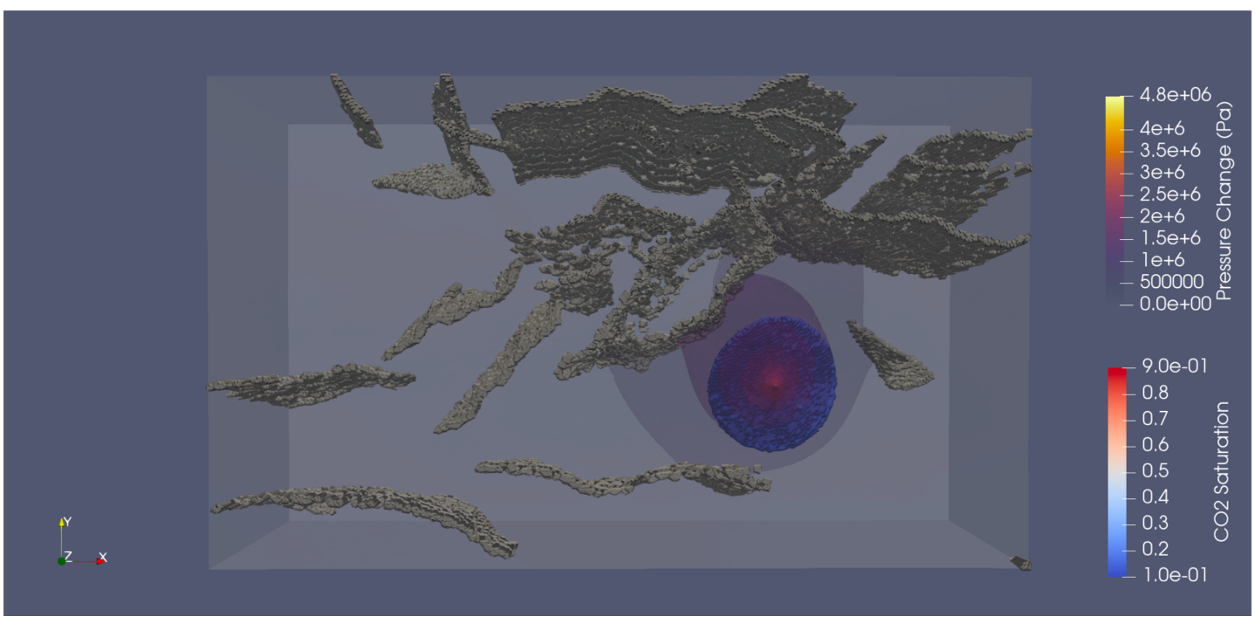

Figure 5. Depleted field simulation results. The extent of the CO_2 plume is shown in blue with the extent of the related pressure plume shown on a scale from black to yellow. Faults are shown in gray. As expected, both the injected CO_2 and its associated pressure front moved in the up-dip direction towards the crest of the four-way structural dome. The greatest magnitude pressure change occurred at the injection site, with a pressure increase of 4.8 MPa. A pressure front of about 1.0 MPa reached the faults near the top of the four-way structure.

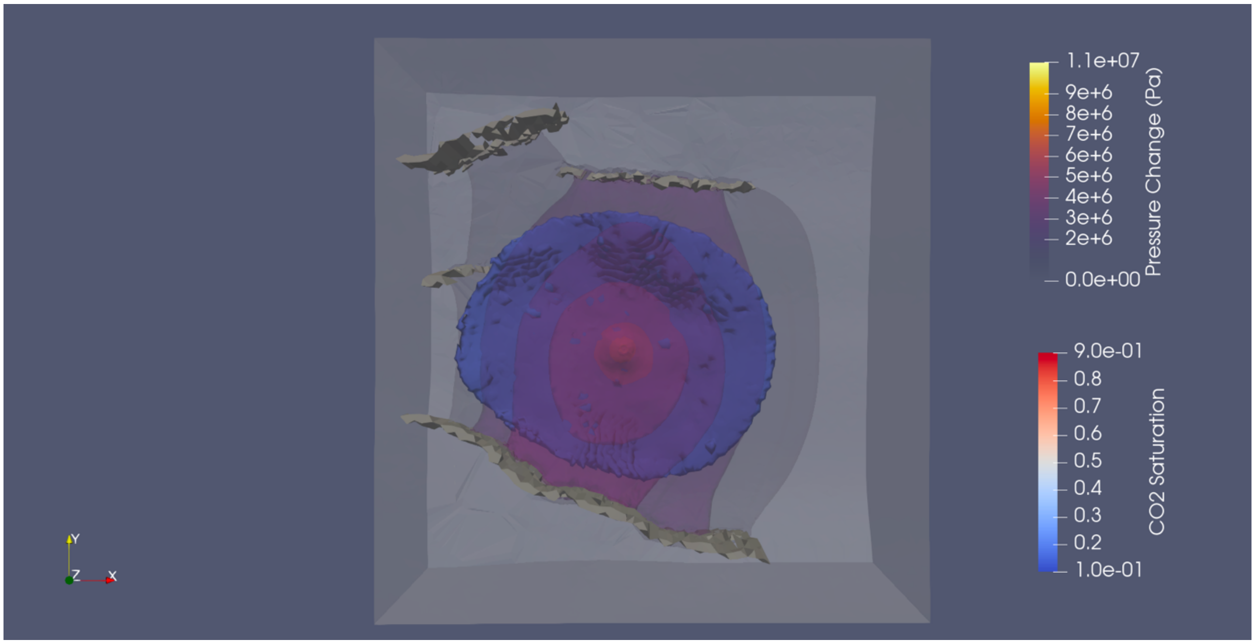

Figure 6. Saline field simulation results. The extent of the CO_2 plume is shown in blue with the extent of the related pressure plume shown on a scale from black to yellow. Faults are shown in gray. As the injection site sits at a local structural low point, injected CO_2 and pressure moved up-dip towards the North and South. The pressure front backs up against the faults, applying as much as 3.3 MPa of pressure increase, which poses risks for pressure-induced alteration.

Discussion

As the simulation results demonstrated that commercial CCS injections at these prospects may be feasible from a technical geologic standpoint, we then investigated the economics and cost of a potential project at these sites. We identified CO_2 sources that are located near our study sites and are eligible for IRC Section 45Q tax credit with a minimum emission rate of 500,000 metric tons of CO2 per year (U.S. Code 26, 2011). We grouped nearby emitters into three distinct clusters, which represent major CO_2 sources that could benefit from CCS development (Figure 7). Altogether, there are 66 facilities with an emission rate of around 115 MMT per annum. In Cluster 1, there are 27 facilities with around 50 MMT annual emissions. Cluster 2 has 17 facilities with 25 MMT total emissions and Cluster 3 has 22 facilities with 40 MMT of total annual CO_2 emissions. As the second cluster is nearest to our prospects, it was selected as the emissions source for our transport and cost calculations.

Within Cluster 2, the Cameron Liquified Natural gas Plant, operated by Sempra energy was identified as the ideal CO_2 source for a hypothetical CCS project at our study site as CO_2 emitted from operations at an LNG plant will be cleaner and cheaper to capture than plants that produce dirty CO_2. In addition, the annual emissions from this plant exceed 2.5 MMT, ~2.62 MMT of CO_2 in 2021, which matches the injection targets that were used for simulation. To plan an effective transportation route from our targeted LNG plant to both of our potential CCS reservoirs, we employed a combination of geospatial methods, including Distance Accumulation and Optimal Path Analysis. Using these methods, we were able to plot the most effective and direct route from the source to our two reservoirs while ensuring the avoidance of sensitive and protected environmental areas, as well as land with significant cultural importance. Based on these optimal paths, the projected pipeline distance from our source to the four-way trap reservoir was ~104 km, while the pipeline distance to the saline play was ~128 km. Additionally, based on an annual injection rate of ~2.5 MMT, a pipeline 10 inches in diameter would be suitable for our operation (Abramson et al., 2020).

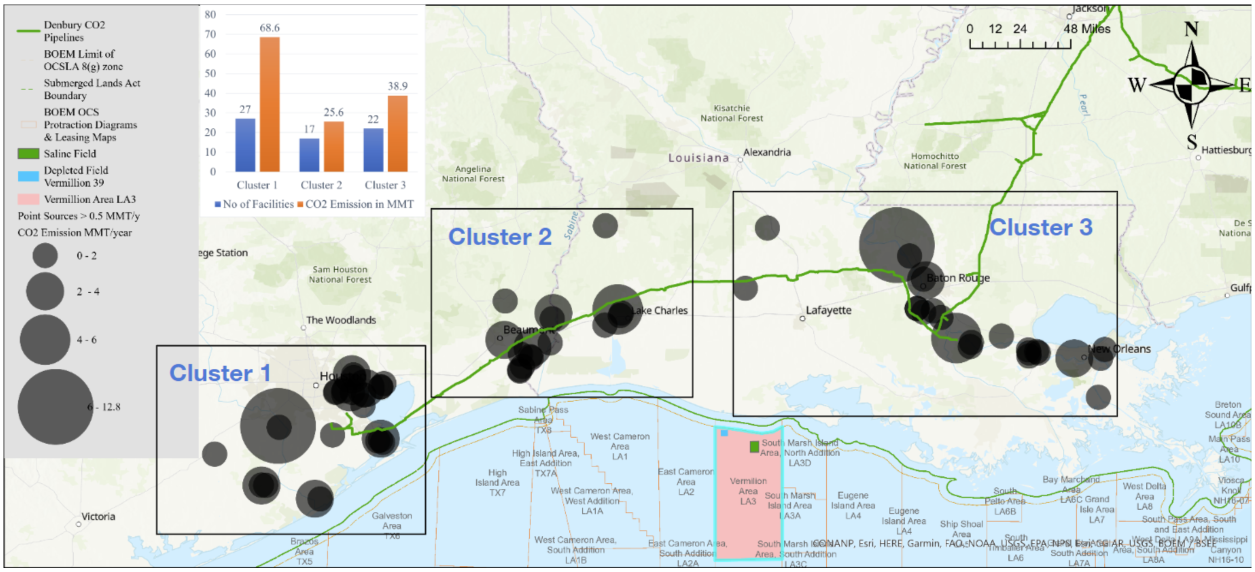

Figure 7. Section 45Q tax credit eligible facilities located near our CO_2 storage prospects and grouped into clusters. Cluster 1 includes major emitters in the greater Houston, TX area, Cluster 2 contains emitters in the Beaumont, TX and Lake Charles, LA area, and Cluster 3 comprises the Louisiana Chemical Corridor (Emissions data is from the EPA GHG reporting program, 2022).

Finally, the project team performed a comprehensive cost estimation to provide an overview of the financial structure, cash sources, and major expenses associated with capturing and storing 50 MMT of CO2 over 25 years using the FECM/NETL cost models (NETL, 2023; NETL, 2017) (Figure 8). The project timeline spans 100 years including the operational and post-injection site care periods of the project. Regarding profitability of the project, around 89% of revenue, $4,250,000 USD, is expected from the 45Q tax credit with an 85 USD/tonne rate. The remaining portion of the project will be financed through debt and equity totaling capital of around $5.2 billion USD. Of the total project cost of 4.3 billion, 16% is allocated to capturing CO_2 at a rate of $14 USD per tonne of (Abramson et al., 2020). Around 37 % of the cost is dedicated to the capital and operations expenditure for CO_2 storage infrastructure. Around 4% of the cost is allocated to transport pipeline construction and operations of 128 km length and 10 inches in diameter. The remaining considerable costs include payments on debt and tax obligations. After accounting for all expenses and revenue sources, the project is expected to produce a profit of $855,954,466.21 USD or 16.36% of the total revenue.

Project Timeline		
	Duration (Yrs)	Calendar Years:
Site Screening	1	2025 - 2025
Transport Pipeline Permitting and Construction	5	2025 - 2030
Site Selection & Site Characterization	3	2026 - 2028
Storage Permitting & Construction	2	2029 - 2030
Operations	20	2031 - 2050
PISC and Site Closure	50	2051 - 2100

Category of Cash		
Sources of Cash		
Revenues for Storing CO2 from 45Q	$4,250,000,000.00	81.22%
Cash withdrwls fr Trust Fnd/Escrow Acct	$ 896,043,894.85	17.12%
Debt Proceeds	$ 86,897,393.49	1.66%
Total Cash from Sources	$5,232,941,288.34	100.00%
Uses of Cash		
Capture Cost	$ 700,000,000.00	15.99%
Storage CAPEX	$1,048,367,351.75	23.95%
Storage OPEX	$ 552,085,403.31	12.61%
Transport CAPEX	$ 111,886,654.50	2.56%
Transport OPEX	$ 65,680,888.99	1.50%
Payments on debt interest	$ 13,564,016.42	0.31%
Payments on debt principal	$ 81,049,475.07	1.85%
Tax Bill	$1,115,878,391.65	25.49%
Cash paid into Trust Fnd/Escrow Acct	$ 688,474,640.44	15.73%
Total Uses of Cash	$4,376,986,822.13	100.00%
Cash Flow to Owners	$ 855,954,466.21	16.36%

Annual Average CO2 Mass Flow Rate	2.5 MMT
Total tonnes of CO2 for project	50 MMT
Length of pipeline	128 Km or 79.5 mile
Nominal Pipe Diameter or Pipe Size	10 in
Cost per tonne of Transportation	$ 3.55
Cost per tonne of Capture	$ 14.00
Cost per tonne of Storage	$ 32.01
CAPEX per mile of pipeline	$ 1,407,379.30
OPEX per mile of pipeline	$ 826,174.70
OPEX per mile of pipeline per year of operation	$ 41,308.74
Total Costs per mile of pipeline	$ 2,233,554.01

Financial Item	Value	Units/ Comments
Percent Equity (remainder is debt)	55.00%	Capitalization
Cost of Equity	12.00%	
Cost of Debt	5.50%	Interest rate
Tax Rate	38.00%	Matches PSFM
Escalation Rate	3.00%	
General and Administrative (G&A) Factor	20.00%	Assessed on all labor costs
Process Contingency Factor	20.00%	Assessed on all monitoring costs
Project Contingency Factor	15.00%	Assessed on all capital costs
Lease bonus	$ 50.00	$/acre
Injection Fee (for lease holders)	$ 0.25	$/tonne
Long-term Stewardship Trust Fund (State)	$ 0.07	$/tonne
Operational Oversight Fund (State)	$ 0.01	$/tonne

Figure 8. Project cost estimates showing an expected net profit of ~$856 million USD.

Conclusions

We propose that the two CCS prospects considered in this study, the depleted petroleum field centered around VR #39 and the saline aquifer field located in VR #55-56 and $67-68 are both highly viable for commercial CO_2 capture and storage projects. Seismic reflection and well data were used to identify suitable reservoir-seal packages in Upper Miocene stratigraphy and numerical modeling and simulation gives strong evidence that these packages could store 50 million metric tonnes of injected CO_2. Furthermore, preliminary cost estimates for capture, transport, and storage of CO_2 at these sites show a high likelihood of profitability. Therefore, we present these two prospects within the Vermilion leasing area of the Gulf of Mexico as prime CCS opportunities that could be developed by commercial interests.

Acknowledgements

Geophysical data for the depleted field study area was provided by Fairfield Geotechnologies through the SEG EVOLVE Carbon Solutions program. The project team would like to thank both Fairfield and SEG for providing data that made this study possible. Furthermore, we would like to thank the SEG EVOLVE program coordinators and mentors for providing guidance during the course of this study.

References

National Energy Technology Laboratory (NETL), 2015, Carbon storage atlas, fifth edition: National Energy Technology Laboratory.

Furre, A.K., Eiken, O., Havard, A., Vevatne, J.N., and Kiaer, A.F., 2017, 20 Years of monitoring CO_2 injection at Sleipner, Energy Procedia, **114**, 3916-3926, https://doi.org/10.1016/j.egypro.2017.03.1523.

Hansen, O., Gilding, D., Nazarian, B., Osdal, B., Ringrose, P., Kristoffersen, J.-B., Eiken, O., and Hansen, H., 2013, Snøhvit: The history of injecting and storing 1 Mt CO2 in the fluvial Tubåen Fm, Energy Procedia, **37**, 3565-3573, https://doi.org/10.1016/j.egypro.2013.06.249.

Alonso, C., Boudreau, L., Cross, K., Keevan, J., Stephens, B., Stradley, S., Trosclai, K., 2022, Identification of tier 1 depleted reservoirs in the Gulf of Mexico: Presented at the AAPG CCUS 2022 Conference, https://www.aapg.org/videos/ccus/articleid/62962/identification-of-tier-1-depleted-oil-and-gas-reservoirs-for-co-storage-in-the-gulf-of-mexico.

Ewing, T. E., and Galloway, W. E., 2019, Evolution of the northern Gulf of Mexico sedimentary basin, *In* Miall, A.D., ed., The sedimentary basins of the United States and Canada, Elsevier, 627-694.

Sarwar, G., 2006, On the origin of mini-basins in the Gulf of Mexico, Gulf Coast Association of Geological Societies Transactions, **56**, 743.

Hentz, T. F., and Zeng, H., 2003, High-frequency Miocene sequence stratigraphy, offshore Louisiana: Cycle framework and influence on production distribution in a mature shelf province, AAPG Bulletin, **87**, 197-230.

Bureau of Ocean Energy Management (BOEM), 2019, Atlas of Gulf of Mexico gas and oil sands data, https://www.data.boem.gov/Main/GandG.aspx. Accessed September 2023.

Rasool, M. H., Ahmad, M., and Ayoub, M, 2023, Selecting Geological Formations for CO2 Storage: A Comparative Rating System., Sustainability, **15**, 6599, https://doi.org/10.3390/su15086599.

Hannis, S., Lu, J., Chadwick, A., Hovorka, S., Kirk, K., Romanak, K., & Pearce, J., 2017, CO_2 Storage in Depleted or Depleting Oil and Gas Fields: What can We Learn from Existing Projects? Energy Procedia, **114**, 5680–5690, https://doi.org/10.1016/j.egypro.2017.03.1707.

Iskandar, U.P., and Usman, U., 2011, CO_2 Storage Capacity Estimation of Depleted Oil and Gas Reservoirs in Indonesia, Scientific Contributions Oil & Gas, **34**.

Rackley, S. A., 2017, 11 - Introduction to geological storage, *in* Rackley, S.A., ed, Carbon Capture and Storage, Butterworth-Heinemann, 285–304, https://doi.org/https://doi.org/10.1016/B978-0-12-812041-5.00011-8.

IEA Greenhouse Gas R&D Programme (IEA GHG), 2009, Long Term Integrity of CO2 Storage – Well Abandonment.

RockWare, 2022, PetraSim User Manual, https://www.rockware.com/downloads/documentation/petrasim/PetraSimManual.pdf.

Jung, Y., Pau, G. S. H., Finsterle, S., and Pollyea, R. M., 2017, TOUGH3: A new efficient version of the TOUGH suite of multiphase flow and transport simulators: Computers & Geosciences, **108**, 2-7, https://doi.org/10.1016/j.cageo.2016.09.009.

Credit for Carbon Dioxide Sequestration, U.S. Code 26, 2011, *§ 45Q*. https://www.govinfo.gov/app/details/USCODE-2011-title26/USCODE-2011-title26-subtitleA-chap1-subchapA-partIV-subpartD-sec45Q. Accessed January 9, 2024.

Abramson E, Mcfarlane D, Brown J., 2020, Transport Infrastructure for Carbon Capture and Storage, Great Plains Institute, https://www.betterenergy.org/wp-content/uploads/2020/06/GPI_RegionalCO2Whitepaper.pdf.

Environmental Protection Agency (EPA), 2022, Facility Level GHG Emissions Data. https://ghgdata.epa.gov/ghgp/main.do. Accessed January 9, 2024.

National Energy Technology Laboratory (NETL), 2023, FECM/NETL CO2 Transport Cost Model Version 4, https://netl.doe.gov/energy-analysis/details?id=d3086f60-278d-4e97-a649-8e4d5ce5e93c/. Accessed 9 January 2023.

National Energy Technology Laboratory, 2017, FE/NETL CO2 Saline Storage Cost Model, https://www.netl.doe.gov/research/energy-analysis/search-publications/vuedetails?id=2403. Accessed 9 January 2024.